Published in final edited form as:

IEEE Trans Appl Supercond. 2012 June ; 22(3): . doi:10.1109/TASC.2011.2178970.

No-Insulation (NI) Winding Technique for Premature-Quench-Free NbTi MRI Magnets

Seungyong Hahn,
Francis Bitter Magnet Laboratory, Massachusetts Institute of Technology, Cambridge, MA 02139 USA

Dong Keun Park,
Francis Bitter Magnet Laboratory, Massachusetts Institute of Technology, Cambridge, MA 02139 USA

Kwangmin Kim,
Francis Bitter Magnet Laboratory, Massachusetts Institute of Technology, Cambridge, MA 02139 USA. He is now with the Department of Electrical Engineering, Changwon National University, Changwon 641-773, Korea

Juan Bascuñán,
Francis Bitter Magnet Laboratory, Massachusetts Institute of Technology, Cambridge, MA 02139 USA

Yukikazu Iwasa
Francis Bitter Magnet Laboratory, Massachusetts Institute of Technology, Cambridge, MA 02139 USA

Abstract

This paper describes and discusses a No-Insulation (NI) winding technique that, based on experiment results of two test NbTi coils, promises to significantly improve stability and ease protection of *high performance* magnets; if applied to those used in marketplace MRI magnets, it may eradicate premature quenches that still afflict these magnets, though much less frequently than in the past. The key idea is that a single turn in an NI winding can, upon a quench, share the copper stabilizers of neighboring turns through turn-to-turn contacts. To demonstrate the main features of the NI technique, two test coils (Φ30 mm) were wound with *insulated (INS)* and *no-insulation (NI)* NbTi wires, respectively. The results presented in this paper include: 1) charge-discharge test results and field analyses showing that the NI field performance is essentially identical to that of the INS coil except a charging delay; and 2) charging test results where coil voltages were measured during critical current tests to imply that the NI coil is charged more stably than its INS counterpart.

syhahn@mit.edu, kkmbest@changwon.ac.kr.

Color versions of one or more of the figures in this paper are available online at http://ieeexplore.ieee.org.

Keywords

MRI; NbTi; no-insulation; premature quench; quench-free; stability

I Introduction

Since the 1980s, commercial MRI (Magnetic Resonance Imaging) magnets, all wound with LTS (low temperature superconducting) wires, i.e., NbTi and Nb3Sn, have been successfully marketed. Major MRI system companies now have over 30 years of experience in production of MRI magnets. As a result, design and construction of LTS MRI magnets has been highly organized and regimented [1].

However, *extremely low thermal stability* (typical enthalpy margin of <10 mJ/cm^3), inherent in these LTS magnets operated at liquid helium (LHe) temperatures still afflicts the magnets, at times causing *premature quenches* when the magnets are first energized at the manufacturer's site. For commercial MRI magnets these quenches translate to unwelcome added magnet costs. Premature quenches, though rarely, occur even at the user site. Although nearly achieved, quench-free operation of LTS magnets still remains a major goal of superconducting magnet engineers since the early 1970s when the first LTS magnets were marketed.

We present here a *No-Insulation (NI)* technique that completely eliminates insulation, metallic or organic, in the LTS windings [2]–[4]. Our primarily experimental results to date have demonstrated that the NI technique appears to ensure totally quench-free operation of an LTS magnet. In an insulated winding, the insulation electrically isolates every turn in the winding and prevents current bypassing through the adjacent turns. To prevent overheating, the conductor in an insulated winding must have enough conductive matrix metal, typically copper, that lowers the overall winding current density. Fig. 1 presents schematic drawings of hexagonal close-packed winding cross sections, (a) insulated and (b) no-insulation. The key idea behind the NI technique is that it enables the current in a local quench zone to spill over to the neighboring turns. This current spillover has beneficial impacts for stability and protection. For stability, it may suppress a local quench from becoming a global quench. For protection, it will reduce the matrix current density in a quenched zone, slowing down its heating rate, which in turn prevents overheating of the quenched zone. Also, the absence in the NI winding of insulating material, which is generally of poor thermal conductivity, should facilitate normal zone propagation in a quench event. To demonstrate the beneficial impacts of the proposed NI technique, two test coils were wound with insulated (INS) and NI NbTi wires, respectively, and tested. This paper presents: 1) charge-discharge test results and field analyses based on a proposed circuit model, which shows that the NI field performance, except its delayed charging rate, is essentially identical to that of the INS coil; and 2) stability test results, through coil terminal voltage measurement performed during critical current tests, to show that the NI coil is more stable than its INS counterpart.

II. Construction of NI and INS Coils

A. Conductor and Winding

Two NbTi coils each having 30-mm winding diameter were wound with INS and NI NbTi wires, respectively. Diameters of the INS and NI wires are 0.178 mm and 0.203 mm, respectively, while their copper-to-superconductor ratio is same: 1.3. Fig. 2 shows: (a) dimensions of a bobbin used for both NI and INS coils; and (b) a picture of the NI coil of which winding diameter, height, and number of turns are identical to those of the INS one. Consequently, the differences of inductance and center field between two magnets are less than 1%. But, the peak field in the NI coil at an operating current of 1 A is 18.9 mT which is 7.4% larger than that of the INS one, 17.6 mT. This difference in peak field may explain the difference in the coil critical currents (at 4.2 K with a 0.1-μV/cm criterion), 46 A (NI) vs. 50 A (INS). Both coils were wound dry, i.e., no epoxy. Table I summarizes key parameters of the two test coils.

B. Equivalent Circuit Model

Fig. 3 shows an electrical circuit diagram of the test setup which consists of a DC power supply, the test coil in cryogenic environment (shaded box), a shunt resistor (R_{shunt}), and a switch (SW). Without insulation, current can flow through turn-to-turn contact in radial and axial directions as well as through its original spiral path in azimuthal direction. This anisotropy of an NI coil is modeled in the shaded box in Fig. 3, with three components: L_{LTS} (test coil self inductance); R_θ (azimuthal resistance chiefly of the wire matrix metal and the superconductor flux-flow represented by index); R_C (characteristic resistance of the test coil that chiefly originates from radial and axial contact resistances). For operation below coil's critical current, i.e., superconducting, R_θ may be considered zero. Using the index model [5], R_θ may be expressed by (1) where l_c, E_c, n, I_θ and I_c are conductor length, the critical voltage criterion (0.1 μV/cm), index, coil current (or operating current), and critical current, respectively. For the INS coil, R_C may be considered infinite because the conductor is insulated.

$$R_\theta = \frac{l_c E_c}{I_c}\left(\frac{I_\theta}{I_c}\right)^{(n-1)} \quad (1)$$

III. Test Results and Analyses

Two sets of tests, charge-discharge and charging stability, were performed. The specific aims of the charge-discharge tests are two-fold: 1) to investigate any difference of spatial and temporal field performances between NI and INS coils; and 2) to validate the equivalent circuit model in Fig. 3 in order to explain a charging delay of the NI coil. The charging stability tests are intended to demonstrate that the NI coil has better thermal stability than its INS counterpart.

A. Charge-Discharge Tests

With a test coil placed in a bath of LHe, it was charged to a target current of 10, 20, 30, and 40 A at a 10 A/min rate, held at a target current for ~ 30 s, and then discharged. Fig. 4 shows power supply current plots, identical for both NI and INS coils; black open symbols are for the INS coil tests, while blue solid symbols for the NI coil tests. In each test, coil terminal voltages and center fields were measured.

Fig. 5 presents measured axial fields during the tests. Up to 30 A, fields from the NI and INS coils are virtually identical and proportional to power supply currents, except a small charging delay of NI fields. This implies that, when the power supply currents become steady-state, the currents flow through the spiral paths defined by the windings of the NI and INS coils; no currents bypass through the turn-to-turn contacts in the NI coil. However, when the power supply current reaches 40 A, 87% of the NI coil I_c, the NI coil field saturates at 305 mT, which is 98% of the INS coil field, 310 mT. This discrepancy may be explained with the equivalent circuit in Fig. 3: when the NI coil current approaches its I_c, R_θ given by (1) increases slightly and a portion of power supply current starts bypassing through R_C, which results in reduction of the center field.

Fig. 6 shows axial field scans along the NI and INS coil axes from separate tests at 30 A; black squares are the measured NI fields, while red circles and blue dashes are the measured and calculated INS fields, respectively. The finite element method was used to calculate the INS coil fields. Results in Figs. 5 and 6 show that the spatial field distributions of the NI coil and the INS coil are essentially identical for an operating current (I_{op}) below the coil critical current (I_c), which is a typical operating condition of most superconducting magnets.

To investigate the charging delay of the NI coil in detail, voltages were measured during the 30-A charge-discharge test and presented in Fig. 7, where black squares and red circles are for voltages of the NI and INS coils, respectively. The inset shows an enlarged view of each voltage when the charging was completed at t = 180 s. Provided that the voltage delay is exponential and the R_θ is negligible at I_{op} of 30 A, a charging time constant τ_c can be obtained from Fig. 7 as 1.60 s and the R_C may be calculated as 1.0 mΩ by (2), where L_{LTS} is the inductance of the NI coil (Table I).

$$R_C = L_{LTS}/\tau_c - R_\theta \approx L_{LTS}/\tau_c \tag{2}$$

Fig. 8 is an enlarged view of the red dashed section in Fig. 5 when current reached 30 A at t =180 s. Blue triangles, black squares, and red circles stand for power supply current, NI center field (measured), and INS center field (measured), respectively. Using the equivalent circuit in Fig. 3 with R_C and other parameters in Table I, we calculated the axial center field from the NI coil, B_{zc}, using (3) and (4), where α_M is the magnet constant (7.86 mT/A) of the NI coil (Table I). The results are shown with magenta diamonds in Fig. 8. The calculated fields match well to the measured fields, validating the equivalent circuit model in Fig. 3. As expected, no charging delay was observed from the INS coil.

$$L_{LTS}\frac{dI_\theta(t)}{dt} + R_\theta(t)I_\theta(t) = \left\{I_p(t) - I_\theta(t)\right\}R_C \quad (3)$$

$$B_{zc}(t) = \alpha_M I_\theta(t) \quad (4)$$

B. Charging Stability Test

In charging stability tests, each test coil was energized at 10 A/min rate up to its critical current, 46 A for the NI coil and 50 A for the INS coil, and its terminal voltage was measured simultaneously. Fig. 9 presents the test results where black squares and red diamonds are for the respective NI and INS coil terminal voltages. The voltage traces are much smoother for the NI coil than for the INS coil. More importantly, much fewer voltage spikes were generated by the NI coil than by the INS coil; the voltage spikes are in the time range 1–10 ms. Based on typical disturbance energy density spectra for LTS magnets [5], wire motion with energy densities of 3–20 mJ/cm^3 is likely be a primary disturbance source for these voltage spikes but further investigation should be carefully addressed. The test results imply that the NI coil may have better charging stability than the INS coil, which appears to ensure premature-quench-free operation of a NI LTS magnet even without epoxy impregnation.

IV. Conclusion

To investigate feasibility of the NI (No-Insulation) winding technique for NbTi MRI magnets, two test coils were wound with NbTi wires, one insulated (INS) and the other no-insulation (NI), and their field performances were evaluated, experimentally and analytically. Firstly, the charge-discharge test results show that field performance of the NI coil for operating current below critical current was essentially identical to that of the INS, one exception being a charging delay. Our circuit model was consistent with the spatial and temporal field behavior observed in the NI coil. Secondly, the charging test results showed that the NI coil was charged more stably than its INS counterpart, i.e., with the NI technique we may be able to *eradicate* unexpected premature quenches that afflict, though much less frequently than in the past, LTS-based MRI magnets, currently wound with insulated wire. The test results of the NI coil, wound dry without epoxy impregnation, suggest that the enhanced stability of the NI coil may make it unnecessary to epoxy impregnate the winding, a cumbersome but an accepted practice to eliminate wire motion in the insulated winding.

However, for the NI technique to become applicable to marketplace MRI magnets, other issues of technical importance must be addressed. These include, in addition to charging delay studied here, quench-induced internal voltages and unbalanced forces, and magnet protection itself.

Acknowledgments

This work was supported in part by the National Institutes of Health.

References

[1]. Cosmus T and Parizh M, "Advances in whole-body MRI magnets," IEEE Trans. Appl. Supercond, vol. 21, no. 3, pp. 2104–2109, 2011.

[2]. Bailey RE, Burgeson J, Magnuson G, and Parmer J, "Metallic Insulation for Superconducting Coils," U.S. Patent 4 760 365, 7 26, 1988.

[3]. Dudarev AV et al., "Superconducting windings with "short-circuited" turns," Inst. Phys. Conf. ser. No 158 (Proc. EUCAS-97), pp. 1615–1619, 1998.

[4]. Evans D, "Turn, layer, and ground insulation for superconducting magnets," Physica C, vol. 354, pp. 136–142, 2001.

[5]. Iwasa Y, Case Studies in Superconducting Magnets: Design and Operational Issues, 2nd ed. New York: Springer, 2009.

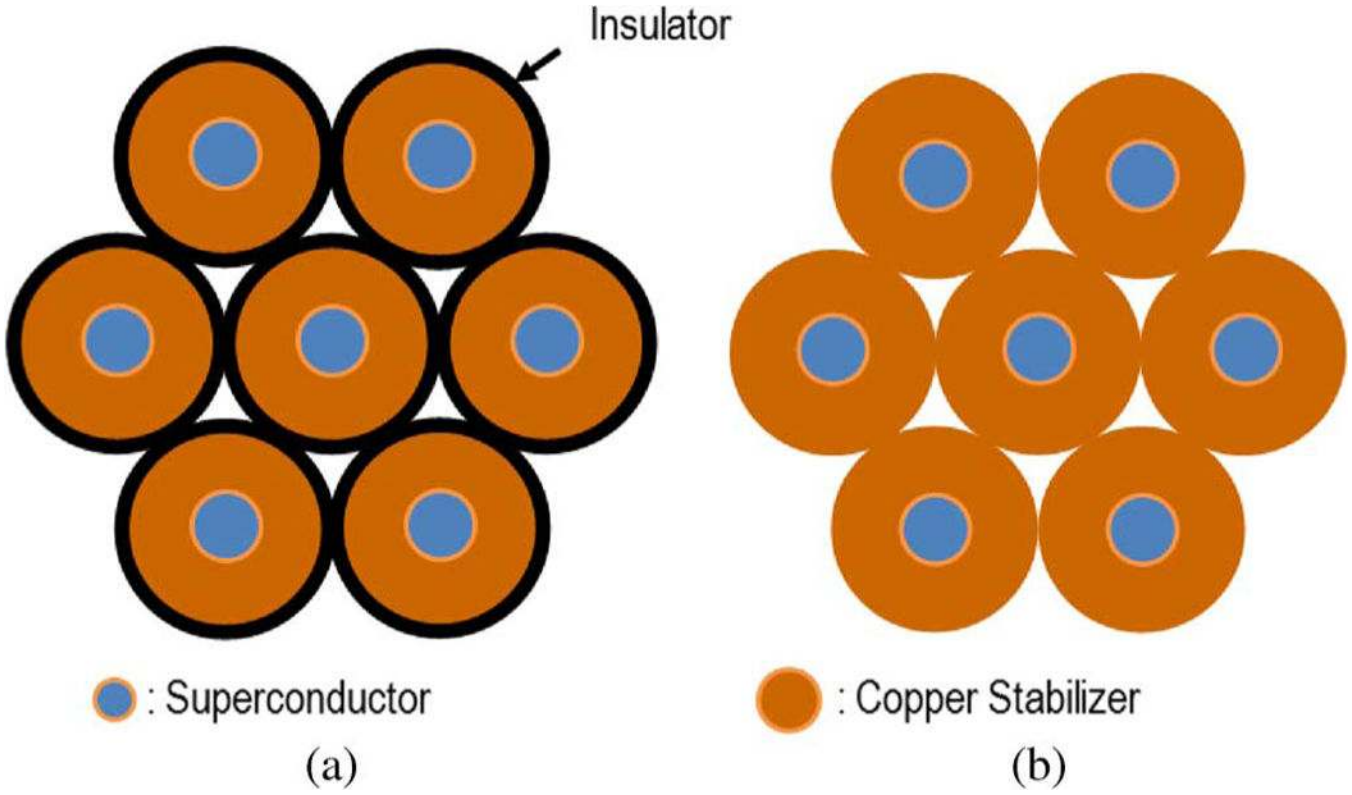

Fig. 1.

Schematics of (a) conventional insulated (INS) and (b) no-insulation (NI) hexagonal close-packed windings. In the NI winding, a single turn shares its copper stabilizer with neighbor turns, benefitting both thermal stability and protection. (a) Insulated (INS) and (b) no-insulation (NI).

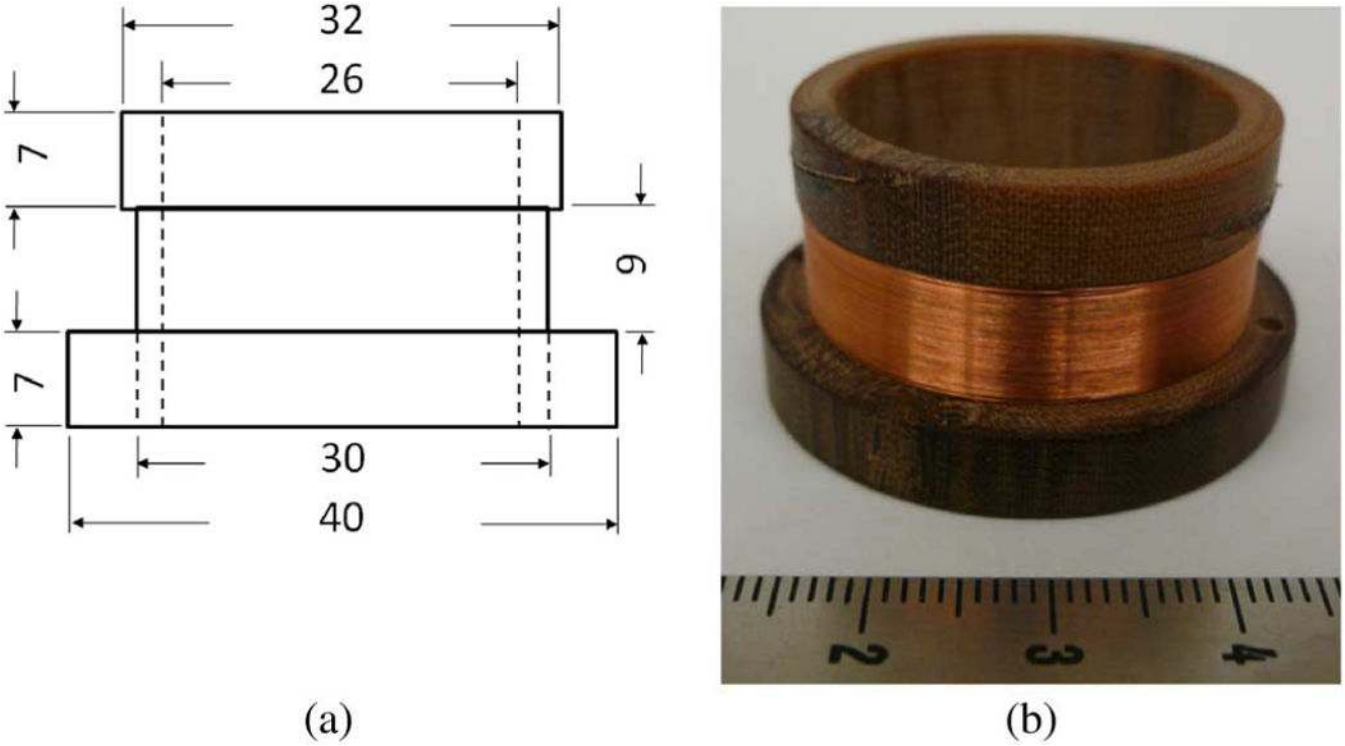

Fig. 2.
(a) Dimensions of the phenolic bobbin used for both NI and INS coils; (b) Picture of NI test coil of which i.d., height, and number of turns are identical to those of INS coil. All units are in mm.

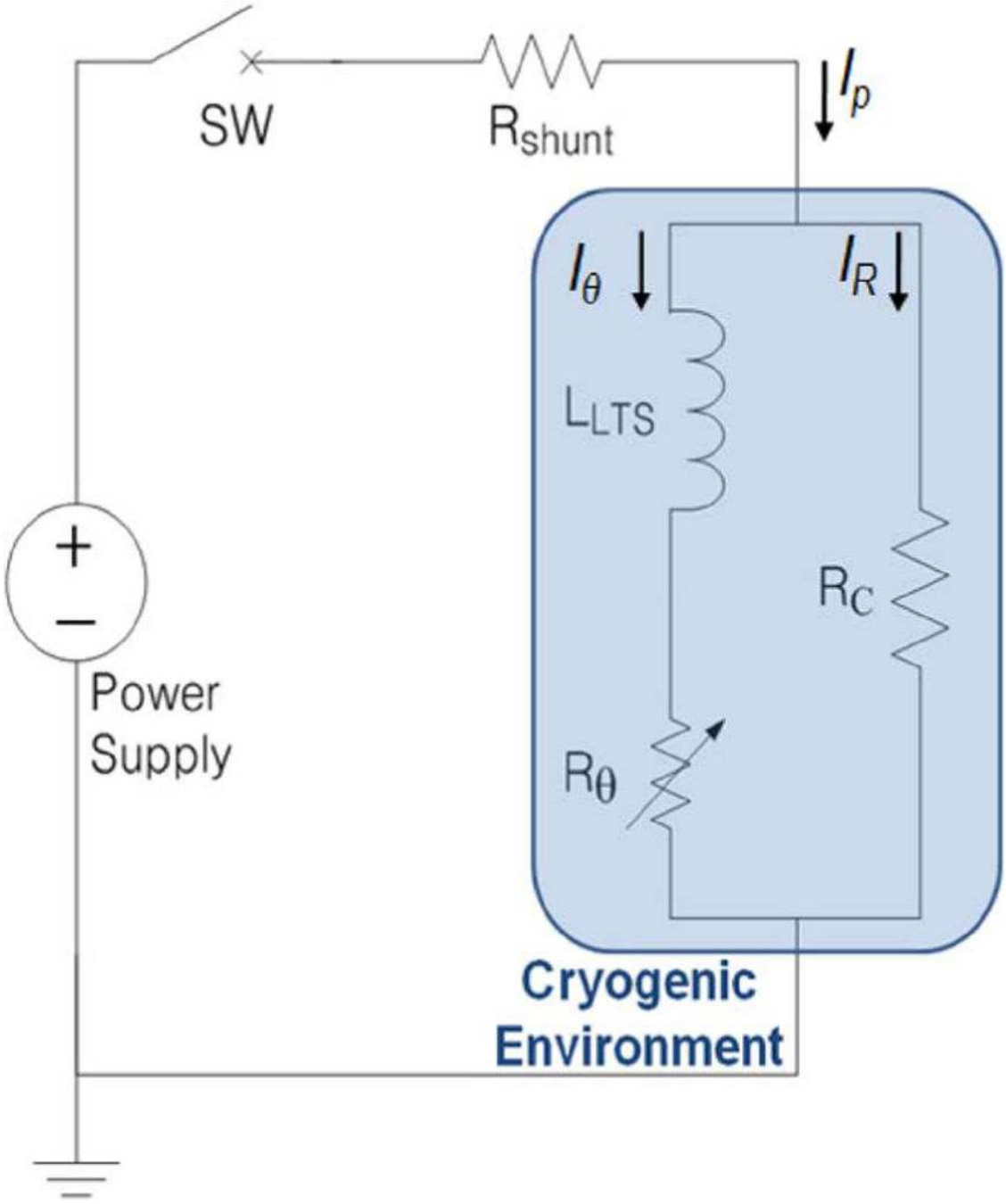

Fig. 3.
Circuit diagram of the test setup with an equivalent circuit model for the NI or INS coil in the shaded box. In the INS coil, R_C may be considered infinite because the conductor is insulated.

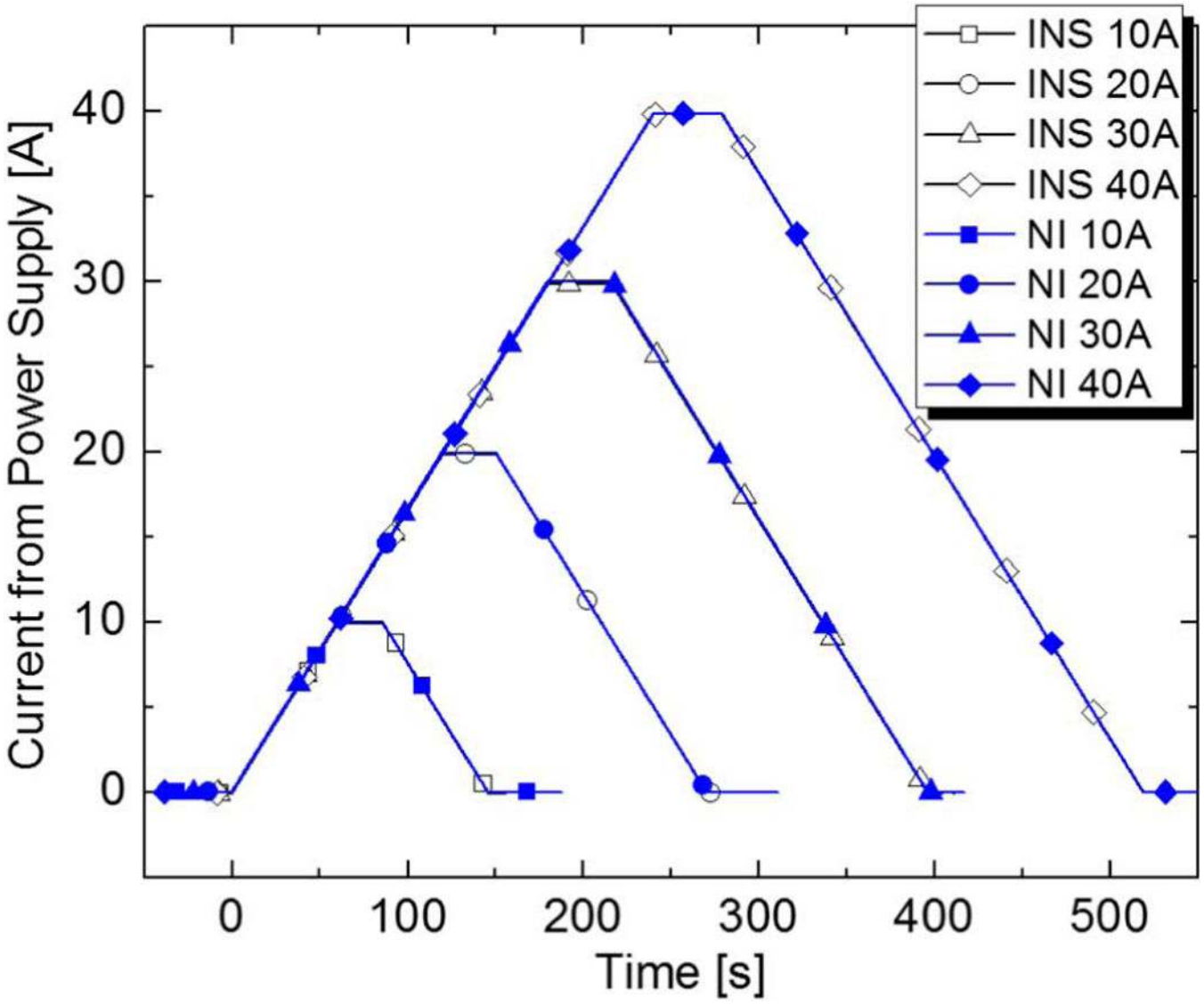

Fig. 4.
Power supply currents for the INS and NI coils during the tests. Time axis is adjusted for ease of comparison.

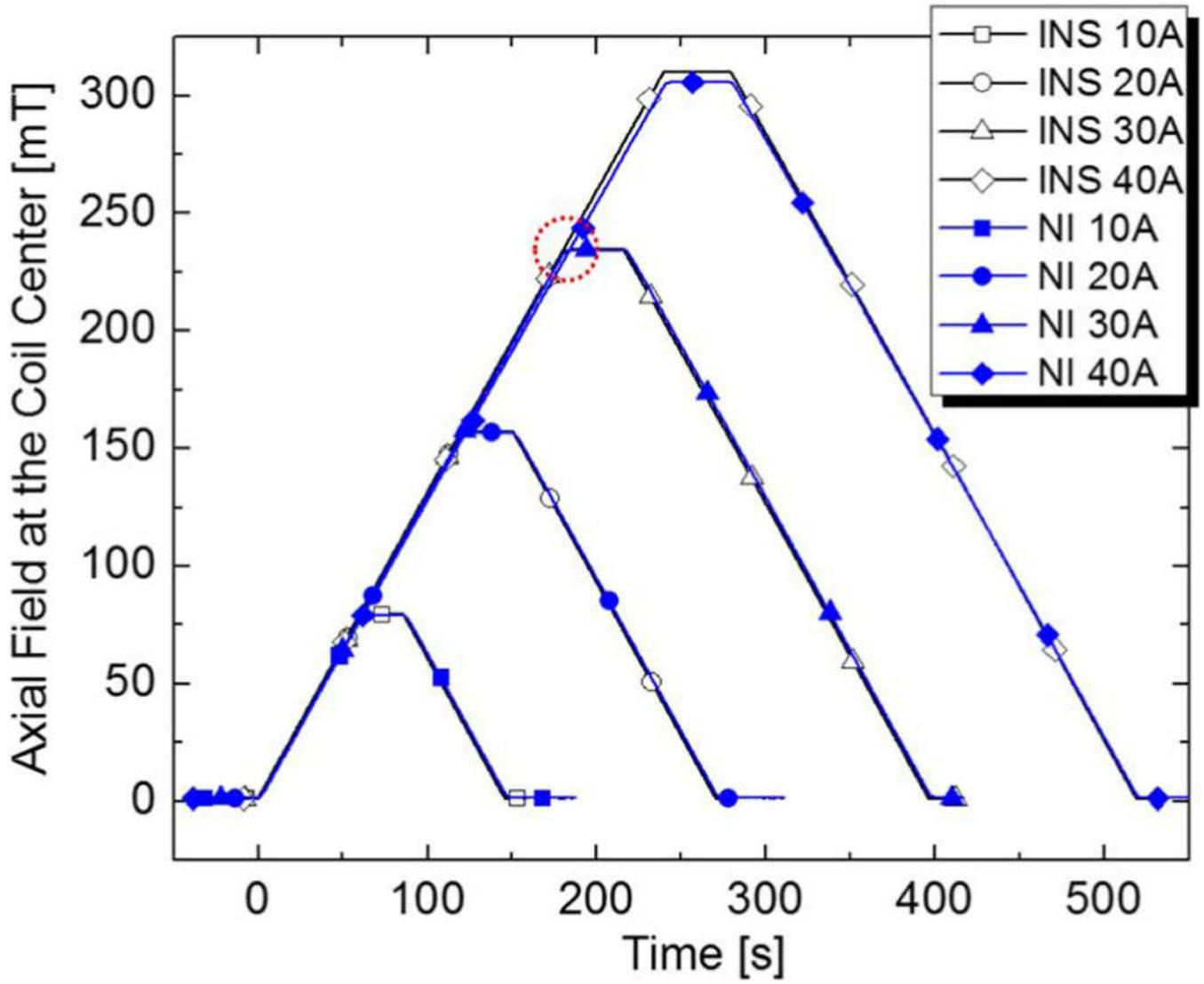

Fig. 5.

Axial center fields of the INS and NI coils at power supply currents of 10, 20, 30, and 40 A. Time axis is adjusted for ease of comparison.

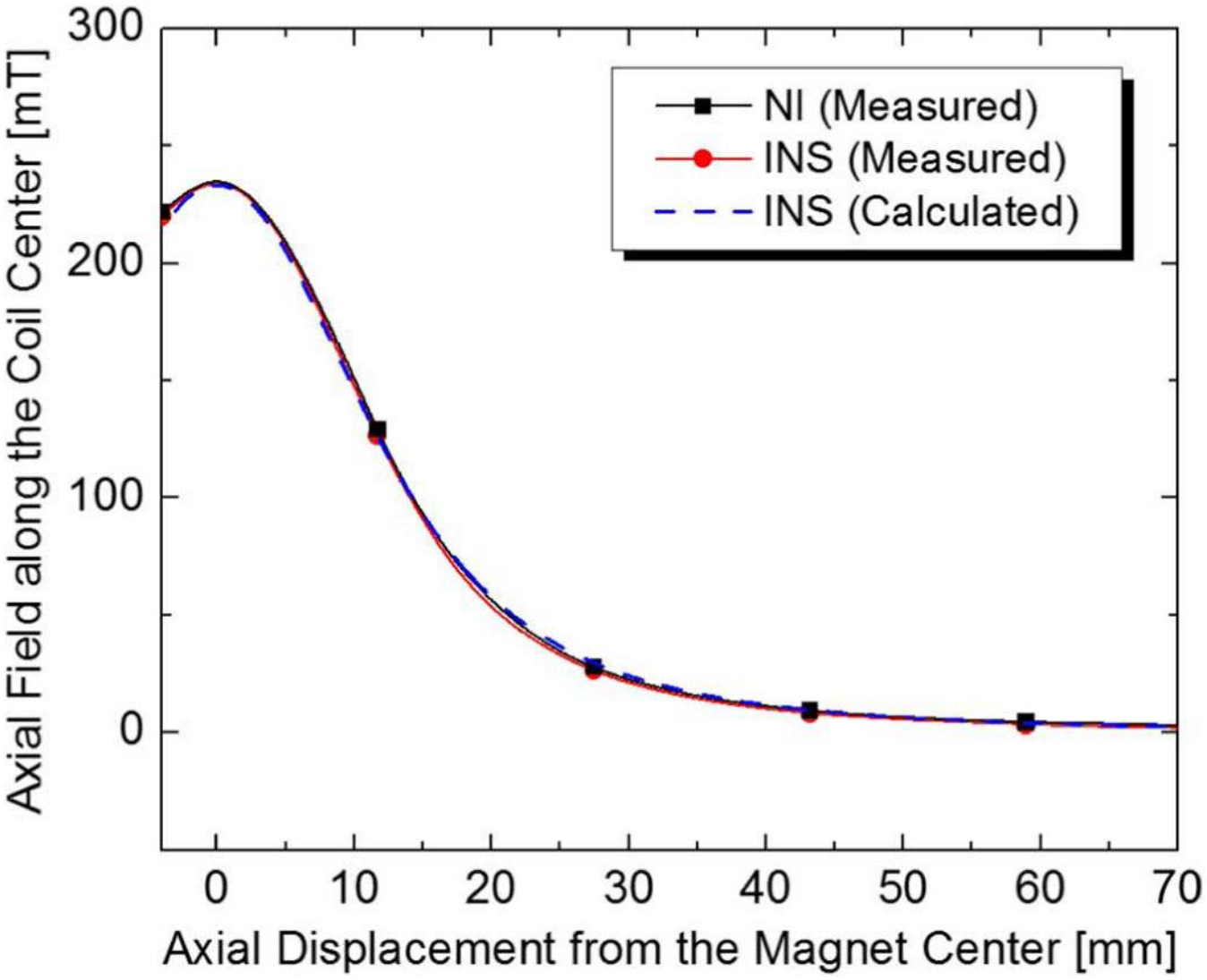

Fig. 6.
Measured and calculated axial field distributions of the NI and INS coils at power supply current of 30 A.

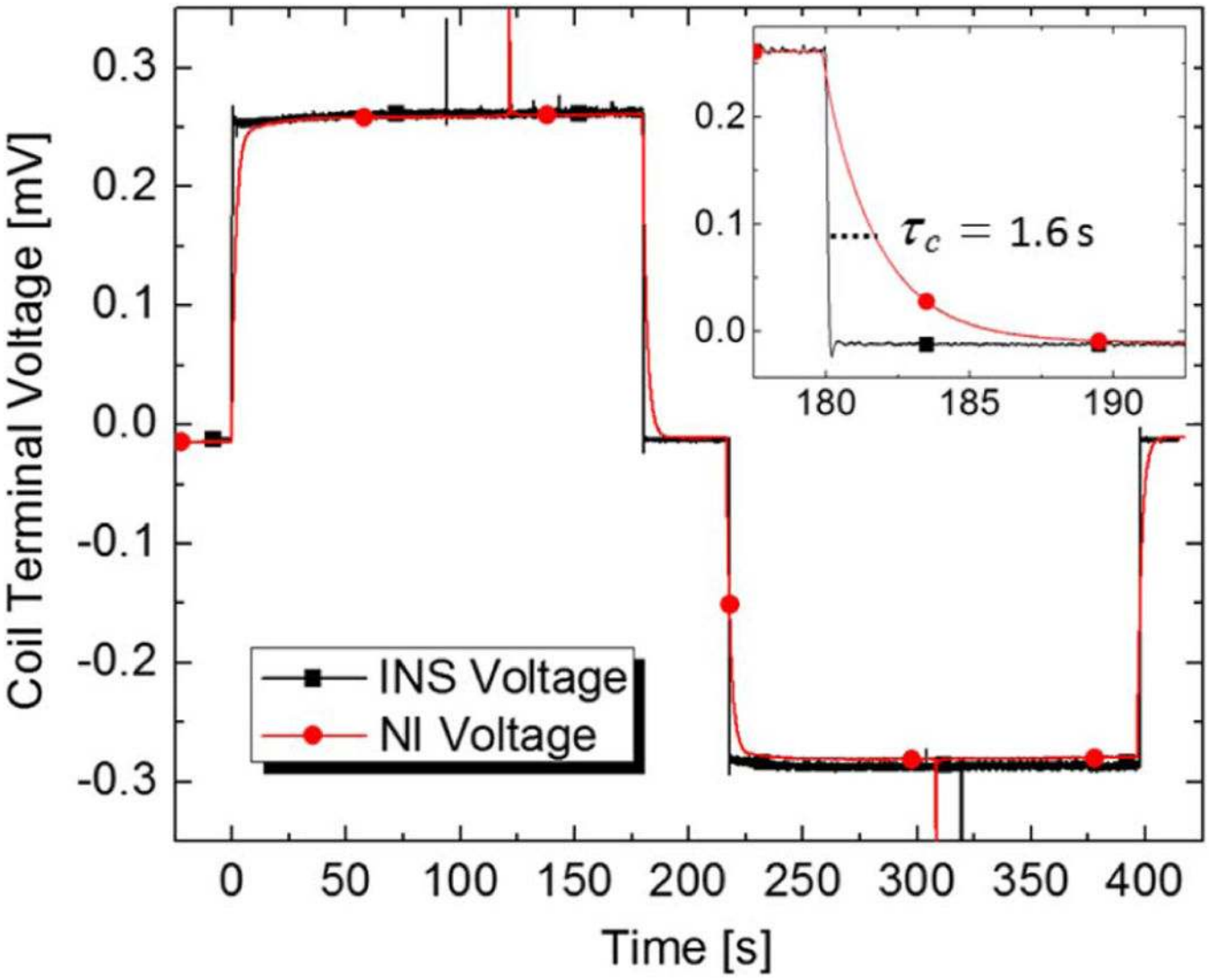

Fig. 7.

Voltages measured during the 30-A charge-discharge test of the NI and INS coils. The inset is an enlarged view at t = 180 s.

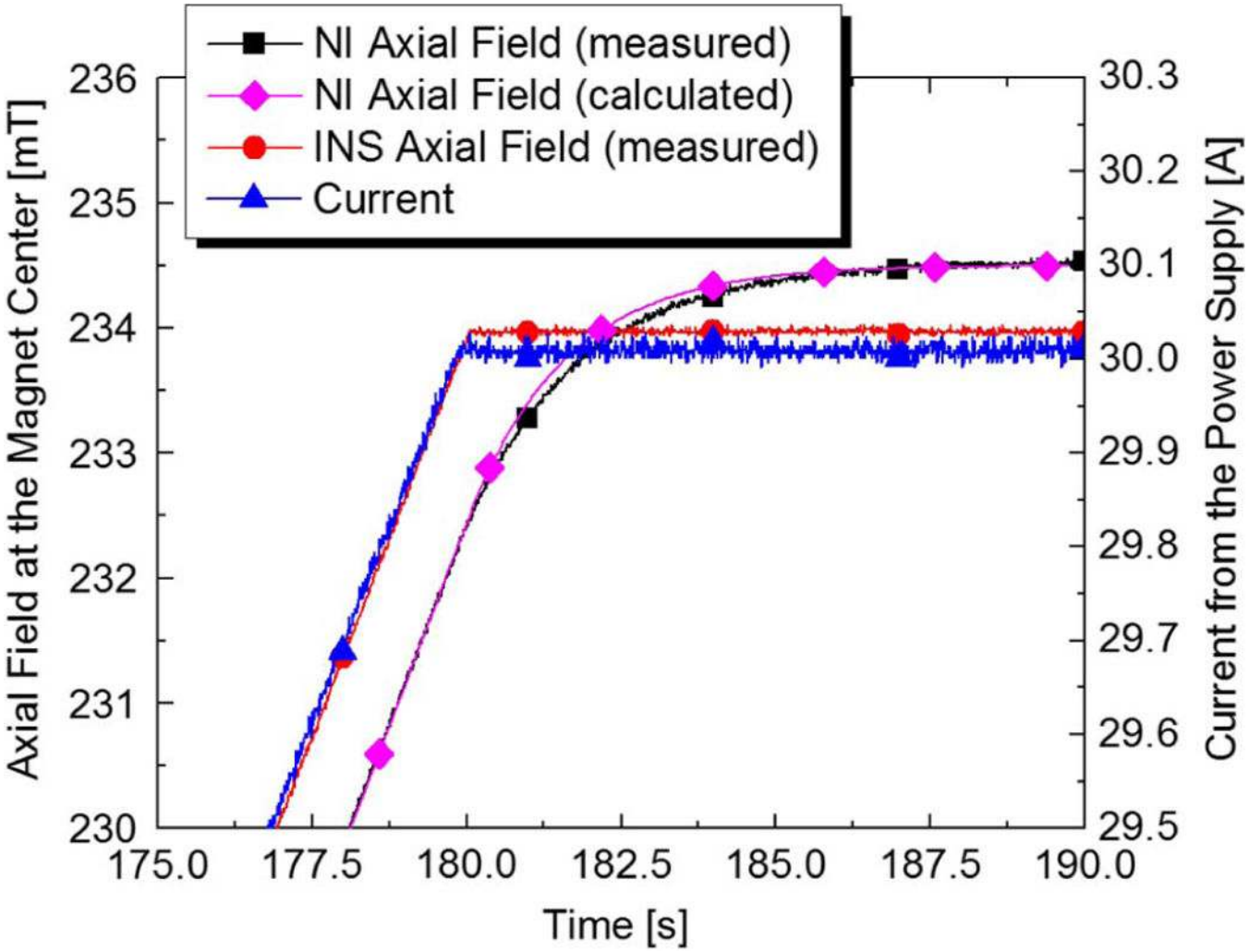

Fig. 8.

Enlarged view of the red dashed section in Fig. 5 when 30-A charging is completed at t = 180 s. The magenta diamonds are for calculated fields from the NI coil using the equivalent circuit in Fig. 3 and the Eqs. (2) and (3).

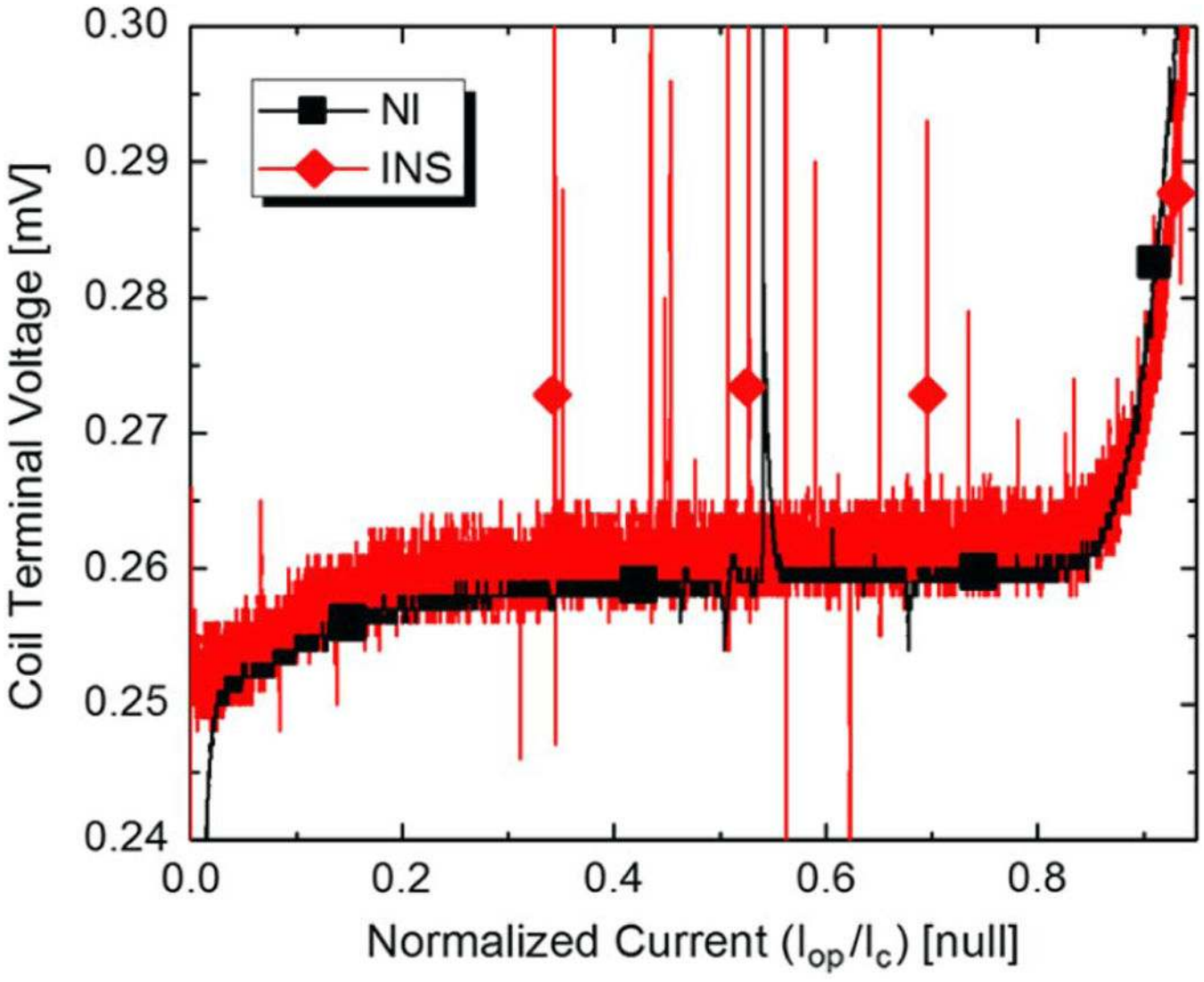

Fig. 9.
Coil terminal voltages during the critical current tests.

TABLE I

KEY PARAMETERS OF NI AND INS COILS

Parameters		NbTi Test Coils	
		NI	**INS**
Conductor			
Diameter	[mm]	0.178	0.203
Cu-to-NbTi ratio		1.3:1	1.3:1
Critical current, I_c	[A]	30 (3T), 20 (4 T)	
Coil			
i.d.; o.d.; height	[mm]	30.0; 31.4; 9.0	30.0; 32.0; 9.0
Number of turns		200	200
Inductance	[mH]	1.595	1.594
Resistance at 300 K	[Ω]	31.0	31.3
Magnet constant (B_{zc}@ 1 A)	[mT]	7.86	7.79
Peak field in the coil @ 1 A	[mT]	18.9	17.5
Coil I_c (0.1-μV/cm criterion)	[A]	46	50
Characteristic resistance, R_C	[mΩ]	1.0	N/A (∞)
Charging time constant, τ_c	[s]	1.6	~0.
winding type		dry	dry